Coordination Chemistry Reviews 254 (2010) 1240–1252

Contents lists available at ScienceDirect

Coordination Chemistry Reviews

journal homepage: www.elsevier.com/locate/ccr

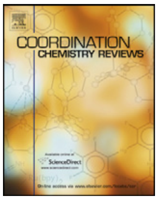

Review

Nonbenzenoid aromatic isocyanides: New coordination building blocks for organometallic and surface chemistry

Mikhail V. Barybin*

Department of Chemistry, The University of Kansas, 1251 Wescoe Hall Drive, 1025 Malott Hall, Lawrence, KS 66045, United States

Contents

ARTICLE INFO

Article history:
Received 4 August 2009
Accepted 3 November 2009
Available online 11 November 2009

Keywords:
Isocyanide
Azulene
Ferrocene
Cymantrene
Homoleptic complexes
Back-bonding
Half-wave potential
Self-assembled monolayers
Gold(1 1 1) surface
Coordination chemistry

ABSTRACT

This review is focused on the emerging chemistry of nonbenzenoid aromatic isocyanides, a relatively new family of aryl isocyanide molecules. Two types of systems are discussed: (1) isocyanoazulenes, for which five archetypal isomeric structures may be envisioned, and (2) η^5-stabilized isocyanocyclopentadienides. So far, the latter are represented by isocyanoferrocene, 1,1′-diisocyanoferrocene, and isocyanocymantrene. In addition, the synthesis and chemistry of the linear 2,6-diisocyanoazulene motif, including regioselective installation and complexation of its –NC termini with controlled orientation of the azulenic dipole, are described. Self-assembly of nonbenzenoid aryl isocyanides and diisocyanides on gold(1 1 1) surfaces is reviewed as well.

1. Introduction

Isocyanides or isonitriles, C≡N—R, are highly reactive, albeit isolable, substances that feature a terminal carbon atom carrying a lone electron pair. This year marked the 150th anniversary since unintended isolation of the first organic isocyanide by Lieke who combined allyl bromide and silver cyanide to yield a liquid with a remarkably repulsive odor [1]. Amid "complaints in the neighborhood about the vile odor", Leike abandoned his experiments with what he thought was allyl nitrile [1,2]. Nearly a decade later, Gautier recognized that the disagreeably smelling compounds generated through alkylation of AgCN were not "nitriles" but rather isomers thereof [2,3]. The pioneering contributions by Ugi in the late 1950s–early 1960s provided a reasonably general synthetic route to organic isocyanides that involved formylation of a primary amine, RNH_2, followed by dehydration of the resulting formamide, RNHCHO [2]. This breakthrough dramatically expanded the pool of documented synthetic isocyanides. Since 1950 [4], a large family of naturally occurring isocyanides has been identified as well [5–7].

During the last 10 years, the commercial availability of isocyanides increased from 12 to 23 compounds, in part, due to growing demand for new substrates in isocyanide-based mul-

---

* Tel.: +1 785 864 4106; fax: +1 785 864 5396.
E-mail address: mbarybin@ku.edu.

0010-8545/$ – see front matter © 2009 Elsevier B.V. All rights reserved.
doi:10.1016/j.ccr.2009.11.002

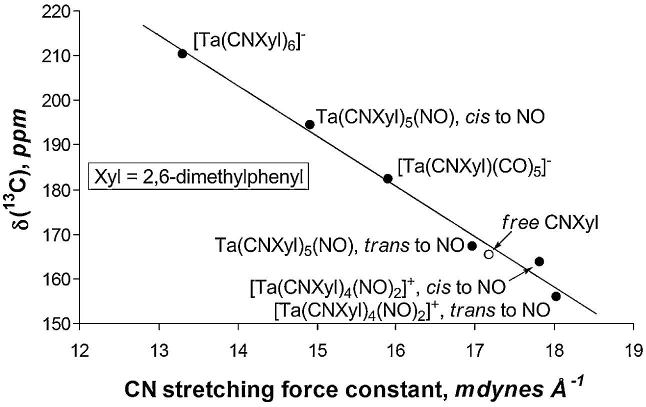

Fig. 1. ^{13}C NMR chemical shifts of the ligating CNXyl carbon atoms plotted vs. the corresponding isocyanide C–N stretching force constants for a series of octahedral tantalum(-I) complexes (the properties of free CNXyl are indicated by an open circle). Adapted with permission from Ref. [22].

ticomponent reactions (MCRs) employed in combinatorial drug discovery [8]. However, most of them are cost-prohibitive if substantial quantities are desired. Of these 23, only 5 possess aryl substituents attached to the isocyanide group. The limited commercial accessibility of isocyanides is, undoubtedly, a consequence of highly demanding restrictions on their handling and storage. Many synthetic isocyanides are thermally unstable and air-sensitive and those of relatively modest molecular weight are extremely malodorous [2,9]. Aryl isocyanides that lack hydrocarbon substituents *ortho* to the isocyanide group are especially prone to deterioration under ambient conditions [9] and often undergo isomerization into the corresponding cyanides at temperatures below 50 °C [10].

The coordination and organometallic chemistry of isocyanides has been at the forefront of numerous advances spanning (a) organic and organometallic synthesis, (b) catalysis, (c) polymer, surface, and materials sciences, as well as (d) diagnostic medicine. A number of these topics have been reviewed [11–20]. As ligands, isocyanides can offer a wide range of steric flexibility through varying the substituent R [21]. In addition, some C≡N—R ligands proved to be quite versatile electronically by virtue of being compatible with both relatively electron-poor and electron-rich transition metal centers [22]. The latter fact is nicely illustrated in Fig. 1, which also reflects the author's choice of "electron-rich/poor" rather than "low/high-valent" terminology in referring to metal ions in this context. Indeed, all complexes considered in Fig. 1 are formally Ta(-I) species. Yet, the vibrational and ^{13}C NMR signatures of their 2,6-xylyl isocyanide (CNXyl) ligands indicate that the isocyanides function primarily as σ-donors in *cis*-$[Ta(CNXyl)_4(NO)_2]^+$, while serving as very strong π-acceptors in $[Ta(CNXyl)_6]^-$ [22].

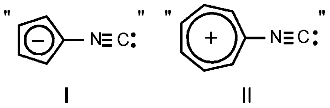

Fig. 2. Hypothetical isocyanocyclopentadienide cation (**I**) and isocyanotropylium cation (**II**).

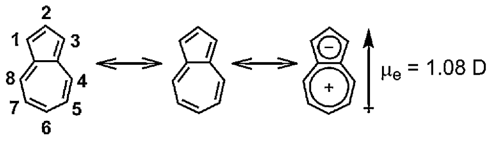

Fig. 3. The resonance structures of azulene and the numbering legend for its scaffold.

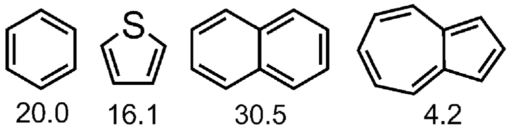

Fig. 4. Aromatic delocalization energies in kcal/mol [39].

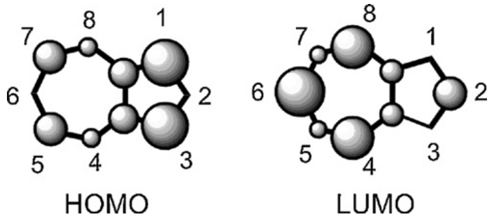

Fig. 5. Schematic drawings of the Frontier molecular orbitals of azulene. The spheres represent squares of atomic orbital coefficients. Reproduced with permission from Ref. [42].

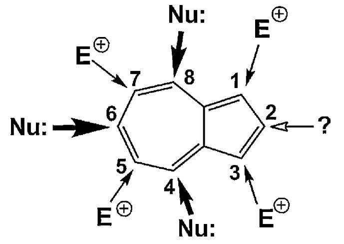

Fig. 6. General strategies for functionalization of the azulene framework.

In general, aryl isocyanides are better suited for accommodating electron-rich transition metals compared to alkyl isocyanides, presumably, due to the possibility of partial delocalization of back-donated electron density into the aromatic rings. As a matter of fact, all six homoleptic isocyanometallates (i.e., complexes of metals in sub-zero oxidation states containing only isocyanide ligands) *isolated* thus far incorporate aryl substituents [22–26]. The "world's record" in this regard belongs to Ellis and Brennessel who have recently reported on the isolation and X-ray structural characterization of $[Fe(CNXyl)_4]^{2-}$ featuring the metal center in the formal oxidation state of -II [23]. The other structurally characterized binary isocyanometallates include $[Co(CNXyl)_4]^-$ (the first example of an isolated isocyanometallate described by Cooper and coworkers) [24], $[Mn(CNXyl)_5]^-$ [25], and $[M(CNXyl)_6]^-$ (M = V, Nb, Ta) [22,26]. Even though very thermally unstable $[Ru(CNXyl)_4]^{2-}$ and $[Ru(CN^tBu)_4]^{2-}$ are not isolable, they were formulated as isocyanideruthenates(-II) by Cooper et al. based on their reactivity with electrophiles [27].

Until the turn of the 21st century, the structural and electronic diversity of aryl isocyanides had essentially been governed by C–H substitution at a benzenoid aromatic ring. This review focuses on the progress made by the author and his colleagues in the synthesis, coordination and surface chemistry of nonbenzenoid aromatic isocyanides, which may be formally regarded as derivatives of presently unknown isocyanocyclopentadienide anion (**I**) and isocyanotropylium cation (**II**) (Fig. 2). These include various isocyanoazulenes, isocyanoferrocene, and isocyanocymantrene. For

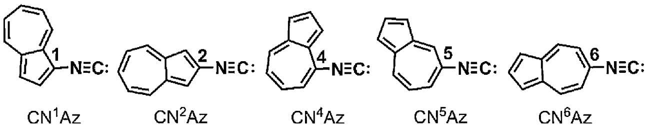

Fig. 7. Five archetypal isocyanoazulenes CN^{x}Az (Az = azulenyl, *x* indicates position of substituent's attachment to the azulene skeleton).

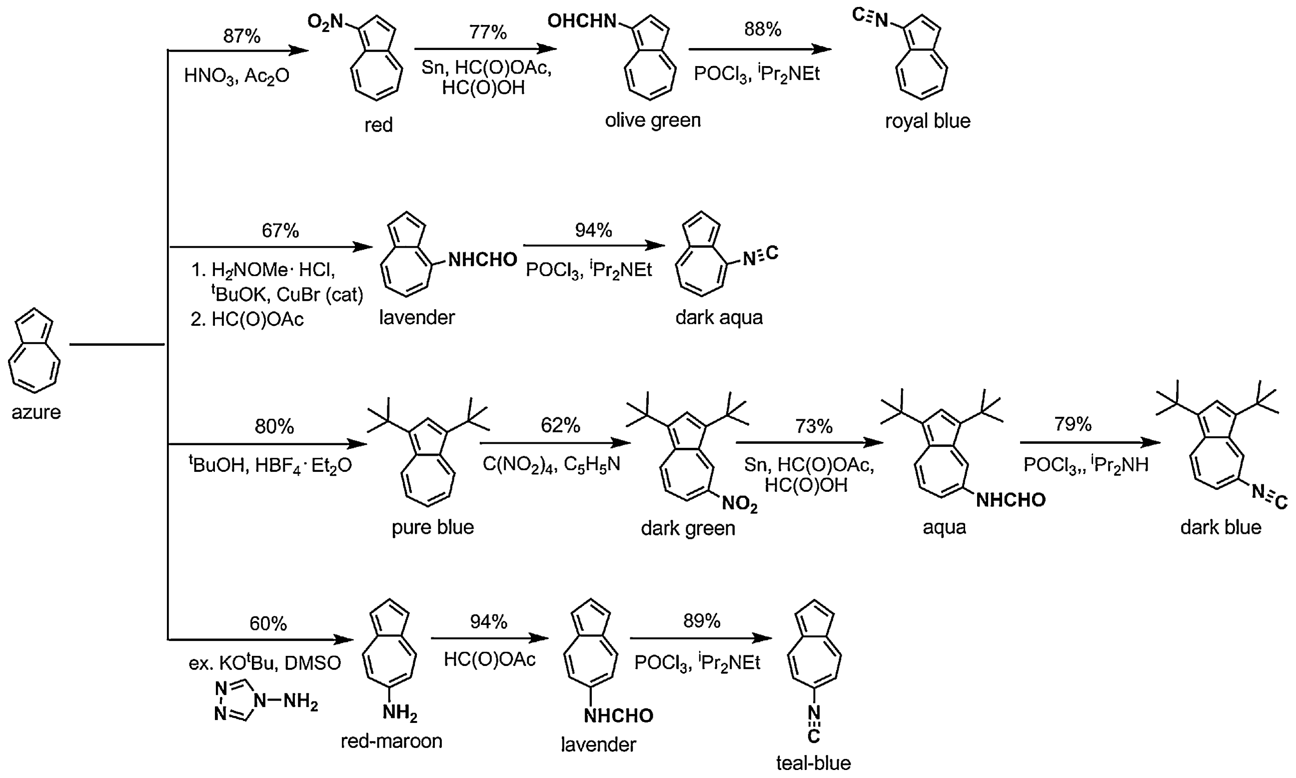

Scheme 1.

the sake of complete review of the subject, the chemistry of 1,1′-diisocyanoferrocene, advanced by other researchers, is briefly surveyed herein as well.

2. The azulenic framework

Azulene is a trivial name for the hydrocarbon bicyclo[5.3.0]decapentaene, $C_{10}H_8$ (Fig. 3). The physical and chemical properties of this polar, nonbenzenoid aromatic species, which are quite different from those of benzenoid aromatics, have been taken advantage of in the development of numerous advanced materials. A few representative examples include conducting polymers [28,29], conducting charge-transfer adducts [30], nonlinear optical chromophores [31–33], optoelectronic switches [34], liquid crystals [35,36], and anion receptors [37,38].

The aromatic stabilization energy of azulene is one-seventh that of its benzenoid isomer naphthalene (Fig. 4) [39] giving in a rather small HOMO–LUMO (HOMO = *H*ighest *O*ccupied *M*olecular *O*rbital, LUMO = *L*owest *U*noccupied *M*olecular *O*rbital) separation for the former. The dark-blue color of azulene is a consequence of the low electron–electron correlation energy associated with the first excited state of this molecule, which corresponds to the HOMO → LUMO transition [40–42]. Unlike naphthalene, azulene

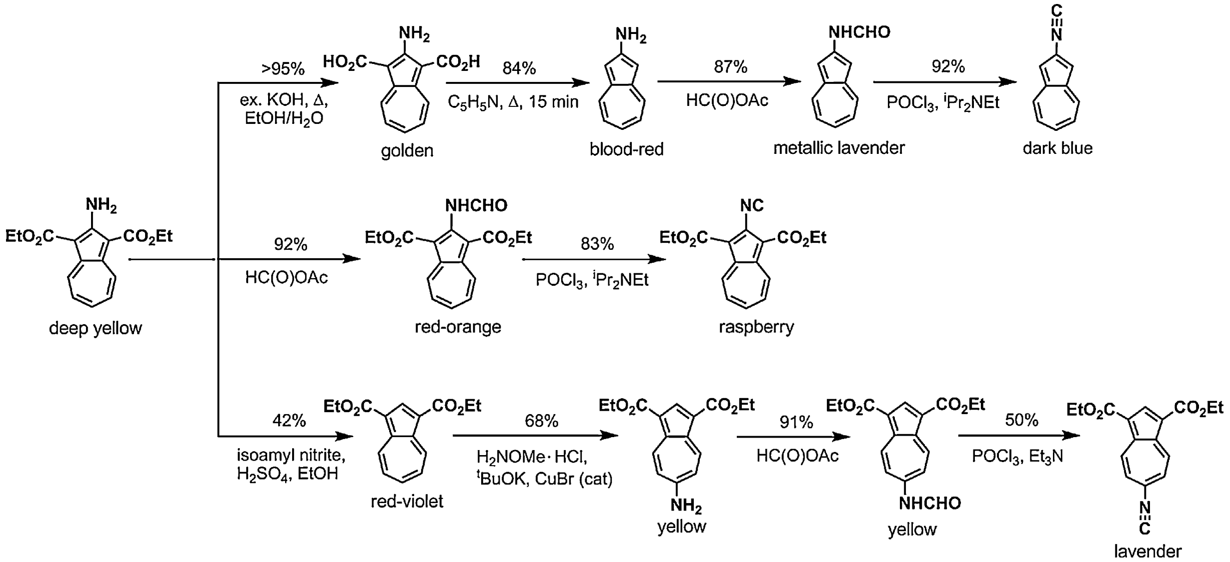

Scheme 2.

features uneven electron density distribution between the two fused rings and its HOMO and LUMO are largely complementary in terms of squares of the atomic orbital coefficients as schematically illustrated in Fig. 5.

Derivatization of azulenes is often accompanied by spectacular color changes because incorporation of an electron-withdrawing substituent at an even-numbered carbon atom or an electron-donating substituent at an odd-numbered carbon atom shrinks the HOMO–LUMO gap of the system, whereas attachment of an electron-donating group at an even-numbered carbon atom or an electron-withdrawing group at an odd-numbered carbon atom widens the HOMO–LUMO separation [40–42]. The general strategies for functionalizing azulene shown in Fig. 6 are largely consistent with the Frontier molecular orbital considerations for the molecule. However, if a 2-substituted azulene is desired, the appropriate substituent must usually be in place before assembling the azulenic skeleton due to the remarkably unreactive C–H bond at the 2-position of the azulene scaffold. Very few ways of direct introduction of a substituent at the 2-position of azulene are known. So far, these are quite limited in scope and involve C–H bond activation through either lithiation or Grignard chemistry [43–46].

According to the Cambridge Crystallographic Database, the majority of azulene-containing organometallics exhibit η^6, η^5, η^4, η^3, and/or η^2 interactions between the azulenic core and one or more metal centers that are often difficult to predict *a priori* [33,47–49]. By embedding azulenic nuclei into polydentate porphyrin ligands to give azuliporphyrins, Lash obtained elegant structures featuring bonding of the metal center to only one carbon atom of the azulenic framework [50]. Prior to our recent work reviewed herein, organometallic/coordination compounds without direct bonding between a metal ion and the azulenic scaffold had been scarce. With few exceptions [50,51], these involve robust 18-electron units containing metal ions "sandwiched" between η^5-cyclopentadienyl and/or η^4-cyclobutadienyl rings [33,52–54]. In 2003, we reported on the first use of isocyanide "alligator clips" to electronically couple azulenes to a low-valent metal center [55]. Shortly thereafter, the complete class of isocyanoazulenes emerged (Fig. 7) [42], which facilitated introduction of the azulenic scaffold as a coordination building block in organometallic and surface chemistry (*vide infra*).

3. Isocyanoazulenes and η^5-bound isocyanocyclopentadienides

3.1. Synthesis and properties

Schemes 1 and 2 summarize the syntheses of various isocyanoazulenes from relatively readily accessible sources [42,56]. Notably, the intermediates 1-nitroazulene [57], 5-nitro-1,3-di-*tert*-butylazulene [58], 6-aminoazulene [59,60], 6-amino-1,3-diethoxycarbonylazulene [59], and 2-aminoazulene [61] were previously described by others but all yields and conditions given in Schemes 1 and 2 reflect the actual experience (including substantial procedure modifications in a few cases) of the author's laboratory. As shown in Scheme 1, CN^1Az, CN^4Az, and CN^6Az are easily synthesized from azulene itself in 2–3 reasonably high-yielding steps. The 1,3-^{t}Bu$_2$-substituted version of CN^5Az can be obtained starting from azulene as well. Since positions 1 and 3 of the azulene framework are significantly more prone to an electrophilic attack than positions 5 and 7 (Fig. 5), it is imperative to block the former before the C–H bond at the 5-position can be activated.

The preparation of CN^2Az (Scheme 2) is somewhat more laborious because the 2-amino group in the starting azulene derivative must be incorporated during the closure of the azulenic nucleus. Fortunately, 2-amino-1,3-diethoxycarbonylazulene can be reliably produced on a large scale from 2-chlorotropone and ethyl cyanoacetate in the presence of NaOEt [62]. In addition to the "parent" CN^2Az, the 1,3-diethoxycarbonyl derivatives of both CN^2Az and CN^6Az are accessible from this 2-aminoazulene.

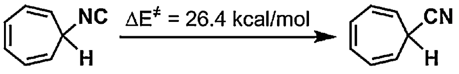

Scheme 3.

The isocyanoazulenes shown in Schemes 1 and 2 can be readily identified by their characteristic ν_{CN} band in IR (2108–2127 cm^{-1}). They are intensely colored, crystalline substances that have surprisingly mild or even barely noticeable odor. With the exception of archetypal 6-isocyanoazulene (which is isoelectronic with elusive 6-azulenyldiazonium cation [59]), all of them are stable under ambient conditions. While solutions of CN^6Az can be handled in air for hours at room temperature without detectable deterioration, its shelf-life in the solid state greatly improves if the compound is kept in an inert atmosphere below −20 °C. Interestingly, α-isocyanonaphthalene, the benzenoid isomer of the "parent" isocyanoazulenes, was described as an air- and thermally sensitive, dark-brown (possibly, due to oligomerization) liquid with a pungent odor [63].

Isocyanoazulenes appear to be robust toward rearrangement into the corresponding thermodynamically preferred cyanoazulenes when subject to heating to at least 70 °C. This is particularly remarkable in light of the facts that (a) aryl isocyanides typically exhibit low barriers to isocyanide → cyanide isomerization [10] and (b) isocyanocyclopolyenes, such as isocyanocyclopentadienes and presently unknown isocyanocycloheptatrienes, were shown theoretically to have quite low barriers to rearrangement into their cyanide isomers [64]. For example, the calculated barrier to the isocyanocycloheptatriene → cyanocycloheptatriene isomerization, shown in Scheme 3, is only about 26 kcal/mol, which implies that this process would occur readily at room temperature [64]. Notably, the formation of an inseparable mixture of isomeric 1-isocyano- and 2-isocyanocyclopenta-1,3-dienes via photolytic degradation of 6-azidofulvenes at −50 °C was invariably accompanied by generation of considerable quantities of 1-cyanococlopenta-1,3-diene [65].

The isocyanoazulenes described above constitute the only class of nonbenzenoid *organic* isocyanides currently known. However, the initial three reports on the first η^5-stabilized isocyanocyclopentadienide, namely isocyanoferrocene, CNFc (Fc = ferrocenyl), date back to the late 1980s [66–68]. The isolated complexes of isocyanoferrocene included $(CNFc)Fe(CO)_4$ and $(CNFc)Cr(CO)_5$ [66–68]. Since then, the chemistry of CNFc remained dormant until 2002 [69]. The apparent lack of interest in this potentially redox-active isocyanide was, undoubtedly, due to its tedious synthesis that produced extremely unattractive yields of the compound. Indeed, (a) the syntheses of aminoferrocene that had been available at the time provided 8–12% yields of H_2NFc starting from ferrocene; (b) formylation of this amine gave 28–46% yields of FcNHCHO depending on the method employed; and (c) dehydration of the latter afforded "variable, nonreproducible (25–90%) yields" of CNFc. This means that the overall yields of isocyanoferrocene starting from the commercially available ferrocene were in the range of 0.6 and 5%!

Between 1999 and 2001, three improved syntheses of H_2NFc were published [70–72]. We had taken advantage of one of these discoveries [70] and, in 2002, communicated a highly reproducible preparation of peach-colored isocyanoferrocene, as summarized in Scheme 4 [69]. The overall yield of CNFc based on the starting ferrocene was 38%, a factor of 8 improvement with respect to the previous best case scenario. The synthesis of the H_2NFc interme-

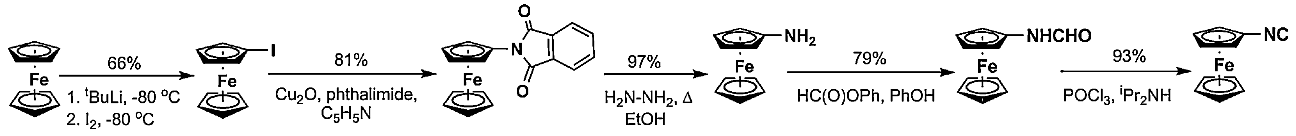

Scheme 4.

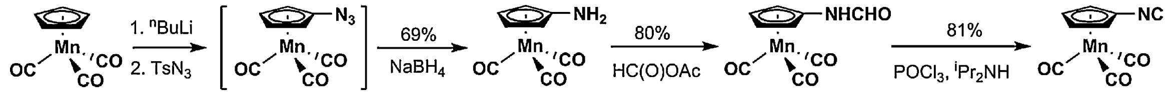

Scheme 5.

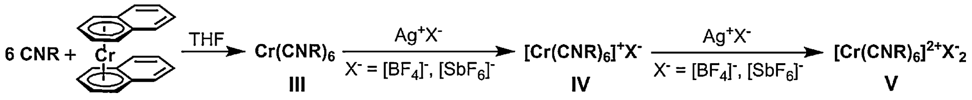

Scheme 6.

diate included in Scheme 4 is essentially that of Bildstein et al. [70]. Notably, it is imperative to avoid using excess $POCl_3$ to achieve practically quantitative dehydration of FcNHCHO to form CNFc [69]. When pure, isocyanoferrocene is reasonably air and thermally stable in the solid state.

Similar to those of ferrocene, derivatives of cymantrene, $CpMn(CO)_3$, are among the most widely used cyclopentadienyl complexes of transition metals [73]. Thus, it was quite reasonable to consider the synthesis of isocyanocymantrene, CNCm (Cm = cymantrenyl $(\eta^5\text{-}C_5H_4)Mn(CO)_3$), in the quest to probe variability of the transition metal fragment attached to the isocyanocyclopentadienyl ring and its effect on the properties of the η^5-stabilized isocyanocyclopentadienide ligand [74]. The challenge of accessing aminocymantrene, which is the most obvious precursor to CNCm, was remarkably reminiscent of the situation with aminoferrocene: the only available preparation called for a laborious six-step procedure (beginning with cymantrene) to afford only 11–26% yields of H_2NCm [74,75].

Fortunately, we discovered a more practical route to aminocymantrene, which involved reacting in situ generated lithiocymantrene with tosyl azide followed by reduction of the resulting azidocymantrene (no isolation necessary) with $NaBH_4$ (Scheme 5) [74]. This essentially "one-pot" approach gave a 70% yield of H_2NCm based on cymantrene. Formylation and dehydration of this amine under standard conditions were uneventful and afforded CNCm in good yield (Scheme 5). Isocyanocymantrene is a pungent, light and thermally sensitive, tan-yellow solid which should be kept in the dark, preferably at about −30 °C, for long-term storage. Nevertheless, this η^5-isocyanocyclopentadienide can be treated as air-stable for practical purposes.

3.2. Homoleptic complexes

As shown in Scheme 6, the isocyanides CNFc, CNCm, CN^xAz (x = 1, 2, 4, 6), 1,3-di-*tert*-butyl-5-isocyanoazulene, and 1,3-diethoxycarbonyl-2-isocyanoazulene react smoothly with 1/6 equivalents of $Cr(\eta^6\text{-}C_{10}H_8)_2$, a labile source of atomic chromium [76,77], to give low-spin d^6 octahedral complexes $Cr(CNR)_6$ (**III**) (e.g., Fig. 8). For R = Fc, Cm, ^{1}Az, ^{2}Az, ^{4}Az, and ^{6}Az, the species **III** were demonstrated to undergo oxidization with one equivalent of AgX (X = BF_4, SbF_6) to afford low-spin d^5, 17-electron, paramagnetic complexes $[Cr(CNR)_6]^+$ (**IV**) with μ_{eff} (25 °C) = 1.71–2.07 μ_B in the solid state [42,74]. Further oxidation of **IV** with AgX provided isolable, low-spin d^4, 16-electron Cr(II) complexes (**V**) in the cases of R = Fc and Cm that have solid state μ_{eff} (25 °C) of 2.76 and 3.01 μ_B, respectively (Scheme 6) [74].

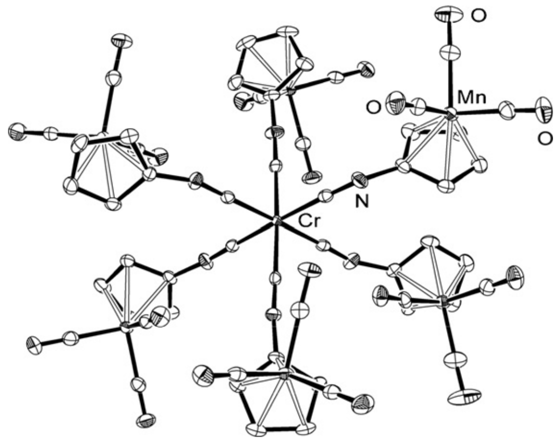

Fig. 8. ORTEP diagram of $Cr(CNCm)_6$ [74].

Crystallographic characterization of the air-stable electrochromic series $[Cr(CNFc)_6]^{0,1+,2+}$ revealed that the Cr–C bonds undergo elongation, while the C–NFc distances shorten upon proceeding from $[Cr(CNFc)_6]^0$ to $[Cr(CNFc)_6]^{1+}$ to $[Cr(CNFc)_6]^{2+}$ (Fig. 9). At the same time, the average C–N–C angle within the isocyanide ligands widens upon successive oxidation of the Cr center. The structural trends akin to those described above for the $[Cr(CNFc)_6]^{0,1+,2+}$ set were also observed for the systems $[Cr(CNPh)_6]^{0,1+,2+}$ [78,79] and $[V(CNXyl)_6]^{1-,0,1+}$ [26] and are consistent with continuous weakening of back-bonding that accompanies the M(0) → M(I) → M(II) oxidations.

	Z = 0	Z = 1+	Z = 2+
Cr-C, Å	1.937(7)	1.972(13)	2.019(17)
C-NFc, Å	1.178(5)	1.160(3)	1.150(5)
C-N-C, (°)	162(4)	171(4)	175(3)

Fig. 9. Trends in the average X-ray metric data for $[Cr(CNFc)_6]^z$ [74].

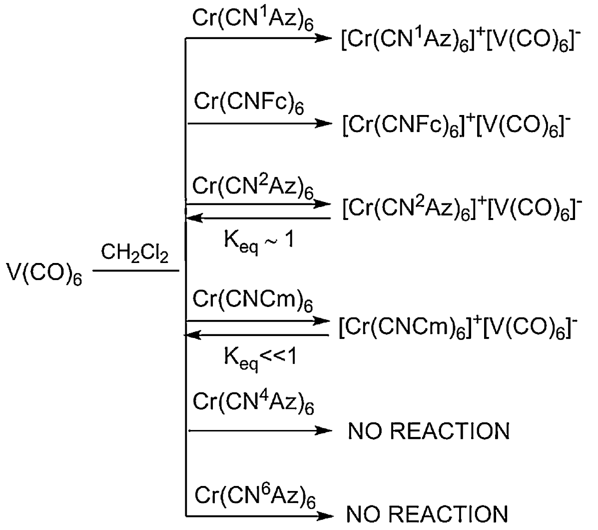

Scheme 7.

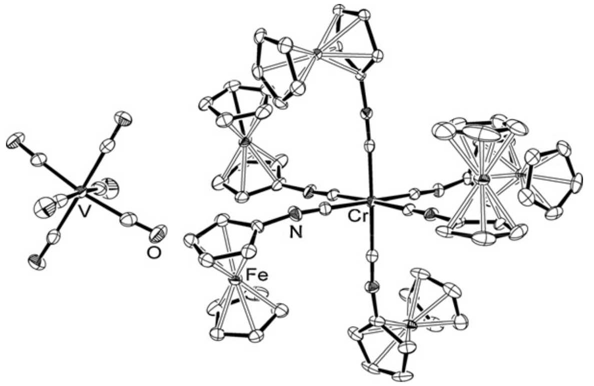

Fig. 10. ORTEP diagram of $[Cr(CNFc)_6]^+[V(CO)_6]^-$. Hydrogen atoms are omitted [74].

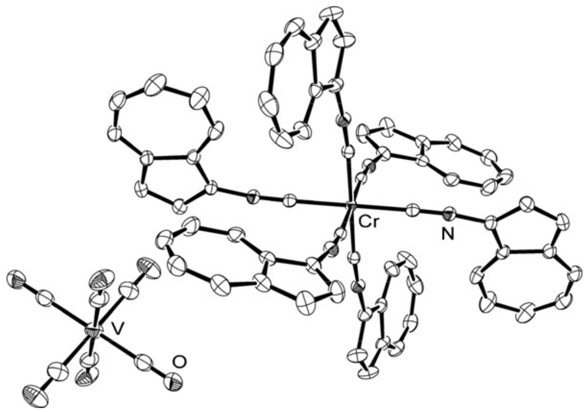

Fig. 11. ORTEP diagram of $[Cr(CN^1Az)_6]^+[V(CO)_6]^-$. Hydrogen atoms are omitted [42].

The zero-valent compounds of the type **III** exhibit markedly different reactivity toward hexacarbonyl vanadium(0), a mild 17-electron oxidant, which allows probing the electron richness of the "$Cr(CN)_6$" core and qualitatively assessing the relative σ-donor/π-acceptor strength of the isocyanide ligands. Among the examples studied (Scheme 7), only $Cr(CNFc)_6$ and $Cr(CN^1Az)_6$ effect the complete formation of the corresponding charge-transfer salts $[Cr(CNR)_6]^+[V(CO)_6]^-$ upon exposure to 1 equiv. of $V(CO)_6$, the Cr(I)/V(-I) nature of which was unequivocally established by X-ray crystallography (Figs. 10 and 11) [42,74]. A stronger oxidant (e.g., Ag^+) is required to irreversibly pull an electron from the electroneutral species $Cr(CNCm)_6$ and $Cr(CN^xAz)_6$ (x = 2, 4, 6) to afford the corresponding Cr(I) complexes (Fig. 12) [42]. Based on the reaction outcomes shown in Scheme 7, the following order of the isocyanide σ-donor/π-acceptor ratios [12] can be suggested: CNFc, $CN^1Az < CN^2Az < CNCm < CN^4Az$, CN^6Az.

The above qualitative considerations are in full accord with the more rigorous cyclic voltammetry studies summarized in Table 1. The data in this table quantify the σ-donor/π-acceptor strength of the isocyanide ligands based on the half-wave potentials corresponding to the reversible ($i_c/i_a \approx 1.0$) consecutive oxidations Cr(0) → Cr(I) and Cr(I) → Cr(II). Notably, $Cr(CNFc)_6$ can be reversibly oxidized by up to 8-electrons on the electrochemical scale [74]. A number of important conclusions can be drawn from the information provided in Table 1.

(1) Contrary to the previous suggestions of electronic similarity between the CNFc and CNMe ligands based on the electrochemistry of $(OC)_5Cr(CNR)$ (R = Fc, Me) [67,68] and the essentially identical Hammett constants for the ferrocenyl ($\sigma_p = -0.180$) and methyl ($\sigma_p = -0.180$) substituents [84], the electronic properties of isocyanoferrocene as a ligand are actually much closer to those of a typical aryl isocyanide rather than methyl isocyanide. Indeed, the $[Cr(CNMe)_6]^0 \rightarrow [Cr(CNMe)_6]^+$ process has the *predicted* $E_{1/2}$ value of −1.67 V against Cp_2Fe/Cp_2Fe^+ in CH_2Cl_2 [85], nearly 0.7 V lower compared to that documented for the $[Cr(CNFc)_6]^{0/+}$ couple under the same conditions. Given the relatively minor role of Cr(dπ) → CNR(pπ*) interaction in $(OC)_5Cr(CNR)$ (R = Fc, Me) due to the presence of five carbonyl ligands, which are stronger π-acceptors than either CNFc

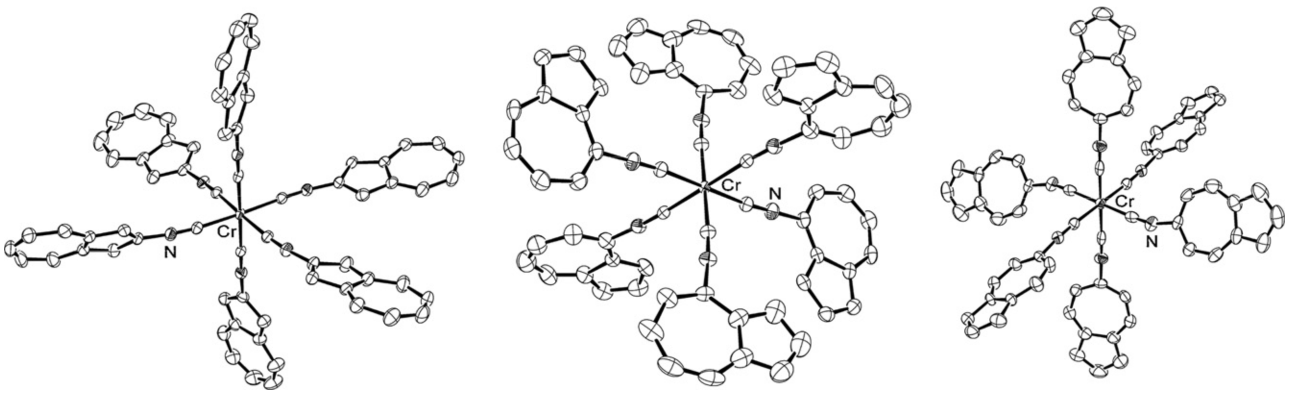

Fig. 12. From left to right: ORTEP diagrams of the cations $[Cr(CN^2Az)_6]^+$, $[Cr(CN^4Az)_6]^+$, and $[Cr(CN^6Az)_6]^+$. Hydrogen atoms and the accompanying $[BF_4]^-$ or $[SbF_6]^-$ counter-ions are omitted for clarity [42].

Table 1
Half-wave potentials for $[Cr(CNR)_6]^{z/z+1}$ couples in $CH_2Cl_2/[^nBu_4N][PF_6]$. The $E_{1/2}$ values are given in volts vs. Cp_2Fe/Cp_2Fe^+.

Couple	Substituent R									
		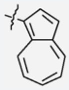		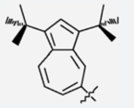	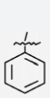	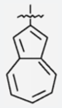	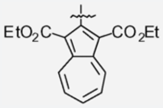	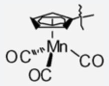	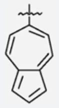	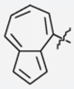
$[Cr(CNR)_6]^{0/1+}$	−1.54	−0.98	−0.97	−0.87	−0.83	−0.69	−0.67	−0.53	−0.49	−0.44
$[Cr(CNR)_6]^{1+/2+}$	−0.77	−0.42	−0.35	−0.29	−0.21	−0.16	−0.14	−0.04	−0.03	+0.02
Reference	[80]	[42]	[74]	[42]	[81,82]	[42]	[83]	[74]	[42]	[42]
					σ-donor/π-acceptor ratio decreases →					

or CNMe, the previously proposed electronic equivalence of the CNFc and CNMe ligands should apply only to their donor characteristics. Notably, our DFT analysis of isocyanoferrocene indicated that its LUMO and LUMO + 2 are particularly suited for delocalizing some of the back-donated electron density beyond the –NC unit [74].

(2) Isocyanocymantrene is clearly a significantly stronger π-acceptor than isocyanoferrocene as evidenced by the large difference in the $E_{1/2}$ values recorded for the $[Cr(CNR)_6]^{0/1+}$ (R = Fc, Cm) couples. Thus, the electronic characteristics of the η^5-stabilized isocyanocyclopentadienide ligand, especially its π-acidity, can be tuned to a substantial extent by varying the metal fragment bound to its ring.

(3) The σ-donor/π-acceptor potential of the isocyanoazulene ligands is a sensitive function of the atom of attachment of the azulenyl moiety. The first oxidation potentials of the $Cr(CN^xAz)_6$ isomers (x = 1, 2, 4, 6) span an interval of greater than half of a volt. Also interesting is the observation that the Cr(0) center in $Cr(CN^4Az)_6$ and the Cr(I) ion in $[Cr(CN^1Az)_6]^+$ appear to be practically identical in terms of their electron richness. The isocyanoazulenes CN^4Az and CN^6Az exhibit the lowest σ-donor/π*-acceptor ratios of all currently known organic isocyanides that feature a purely hydrocarbon substituent.

(4) The two series of the $[Cr(CN^xAz)_6]^{z/z+1}$ (x = 1, 2, 4, 6; z = 0, 1+) redox potentials given in Table 1 serve as quantitative descriptors of the electronic inhomogeneity of the azulenic scaffold. Remarkably, the findings of this organometallic electrochemical assessment correlate quite well with the trend in pK_a's determined for the corresponding azuloic acids, $^xAzCO_2H$, only three of which (x = 1, 2, 6) are known thus far [86] (Fig. 13).

(5) The binary complexes $Cr(CNR)_6$ (R = ^2Az or 1,3-diethoxycarbonyl-2-azulenyl) have almost the same redox properties (Table 1), which implies nearly identical electronic characteristics of their ligands. This is not exceptionally surprising given that the LUMO of azulene lacks contribution from the carbon atoms at positions 1 and 3, while the carbon atom at position 2 does not contribute to its HOMO (Fig. 5). Thus, to a first approximation, neither π-acidic nor σ-donor properties of the CN^2Az ligand should be significantly affected by the 1,3-diester substitution of its azulenic scaffold. A similar argument could, in principle, be made for the 1,3-diester derivatization of CN^6Az and the 2,6-diisocyanoazulene motif (*vide infra*).

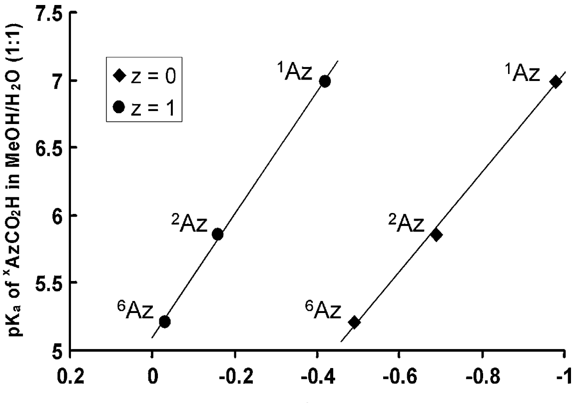

Fig. 13. Correlations between $E_{1/2}$ potentials for $[Cr(CN^xAz)_6]^{z/z+}$ (x = 1, 2, 6; z = 0, 1) couples and pK_a values for the corresponding azuloic acids, $^xAzCO_2H$ (x = 1, 2, 6).

The octahedral, low-spin d^5, paramagnetic complexes of general formula **IV** are EPR-silent but exhibit well-resolved ^1H, ^{13}C, and ^{14}N NMR spectra due to a very short electron–spin relaxation time, T_{1e}, ensured by their approximately degenerate ^2T ground state. Careful analysis of these NMR patterns provided important insight into unpaired spin delocalization within complexes **IV**. For example, in the case of $[Cr(CN^6Az)_6]^+$, relatively large magnitudes and upfield direction of the ^1H paramagnetic shifts (with respect to the signals recorded for the free diamagnetic ligand CN^6Az) observed for the hydrogen atoms at positions 2, 5, and 7 of the ^6Az groups (Fig. 14) indicate presence of excess unpaired spin in the p-orbitals of the corresponding carbon atoms (i.e., #2, 5, and 7). DFT consideration of the nearly degenerate, t_{2g}-like set of the highest occupied molecular orbitals for $[Cr(CN^6Az)_6]^+$ (Fig. 15, top) nicely supports this conclusion and clearly shows that the excess unpaired spin within the π-systems of the azulenyl substituents is, at least in part, a consequence of $Cr(d\pi)\rightarrow CN^6Az(p\pi^*)$ back-bonding interactions [42]. Such interactions within $[Cr(CN^6Az)_6]^+$ can also be illustrated by invoking the classic model for $M(d\pi)\rightarrow L(p\pi^*)$ delocalization as illustrated in Fig. 15, bottom.

4. The 2,6-diisocyanoazulene linker: regioselective installation and complexation of the –NC junctions

The azulenic motif occurs naturally as a defect in certain carbon nanotubes and is thought to be responsible for modulating

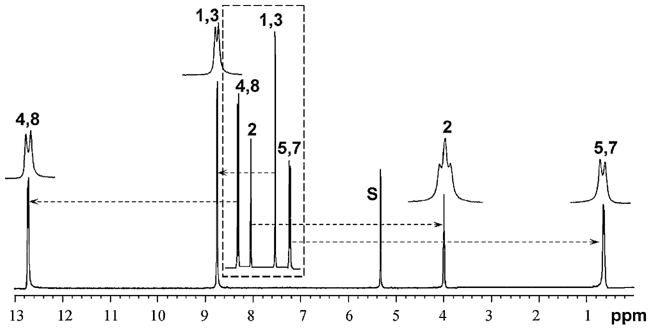

Fig. 14. ^1H NMR spectrum of $[Cr(CN^6Az)_6][BF_4]$ in CD_2Cl_2 at 25 °C. The insert is the ^1H NMR pattern for free CN^6Az in the same solvent. S = residual NMR solvent peak. Adapted with permission from Ref. [42].

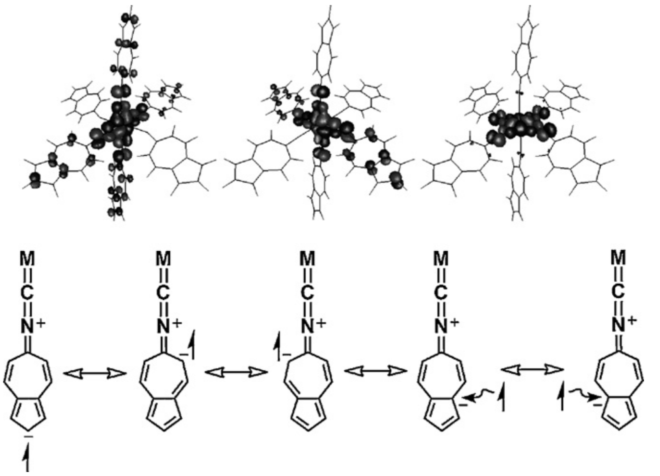

Fig. 15. Top: the nearly degenerate, t_{2g}-like set of the highest occupied molecular orbitals for $[Cr(CN^6Az)_6]^+$, adapted with permission from Ref. [42]. Bottom: resonance structures for the $Cr(d\pi) \rightarrow CN^6Az(p\pi^*)$ interactions within $[Cr(CN^6Az)_6]^+$.

unusual electronic characteristics of these nanostructures [87]. It has been theorized that a framework composed exclusively of carbon pentagons and heptagons could have metallic properties [88]. In 1998, architectures involving a discrete bridging 2,6-azulenic moiety (Fig. 16) was predicted to have intriguing charge transport properties [89]. If an organometallic approach toward experimental realization of such a system is considered, linking two metal termini with the 2,6-azulenic motif directly as shown in Fig. 16 would present an immense synthetic challenge and would probably be impractical due to the likely instability of the resulting species in ambient environment. Given the growing interest in linear aromatic diisocyanides as charge transport mediators for potential nanotechnological applications and our ability to electronically couple the azulenic scaffold to an electron-rich metal center by means of the isocyanide junction, we set out to synthesize the 2,6-diisocyanoazulene motif [90].

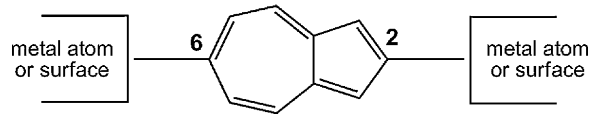

Fig. 16. The hypothetical 2,6-azulenic linker.

Our five-step conversion of 2-amino-1,3-diethoxycarbonylazulene to 2,6-diisocyano-1,3-diethoxycarbonylazulene (**5**) in the overall yield of 51% is shown Scheme 8. The critical steps include (a) changing the electron donating 2-amino group of **1** into the electron-withdrawing formamide (**2**) to activate the azulenic nucleus toward nucleophilic attack at its 6-position by the azide (**2** → **3**) and (b) employing a rather unorthodox reducing combination $FeCl_3/NaI/MeCN$ to effect clean reduction of the azide functionality in **3**, which is accompanied by generation of the I_2 by-product. The 2,6-diisocyanoazulene derivative **5** turned out to be a remarkably air- and thermally stable substance and is storable for many months in ambient conditions without noticeable decomposition. The ν_{CN} stretching frequencies for **5** are observed at 2116 and 2125 cm^{-1} in CH_2Cl_2, which are essentially identical to those documented for CN^6Az and CN^2Az, respectively.

Complexation of both isocyanide junctions of **5** occurred nearly quantitatively upon treating this 2,6-azulenic linker with 2 equiv. $M(CO)_5(THF)$ (M = Cr, W) to give bimetallic adducts **6a**/**b** (Scheme 8). However, when only 0.5 equiv. of the "$M(CO)_5$" synthon was used (Scheme 9), two isomeric monometallic adducts

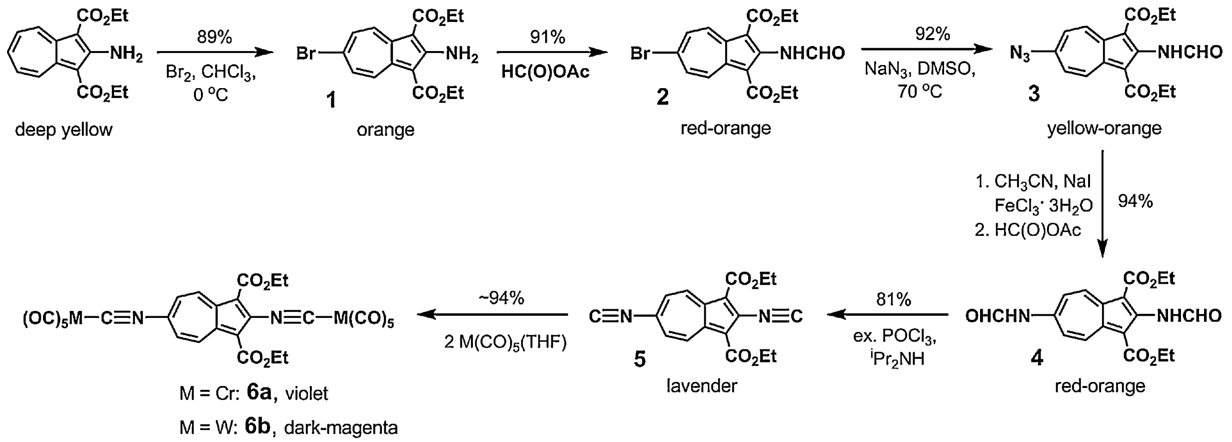

Scheme 8.

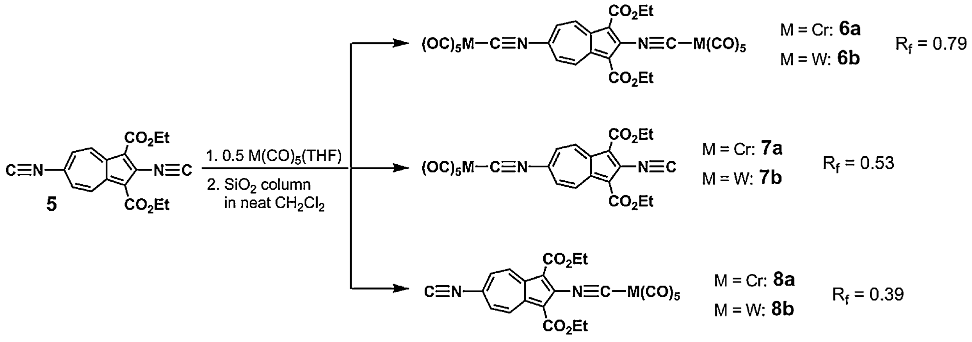

Scheme 9.

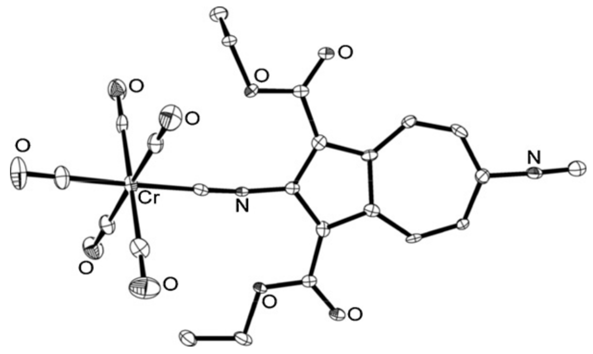

Fig. 17. ORTEP diagram of **8a**. Hydrogen atoms are omitted [90].

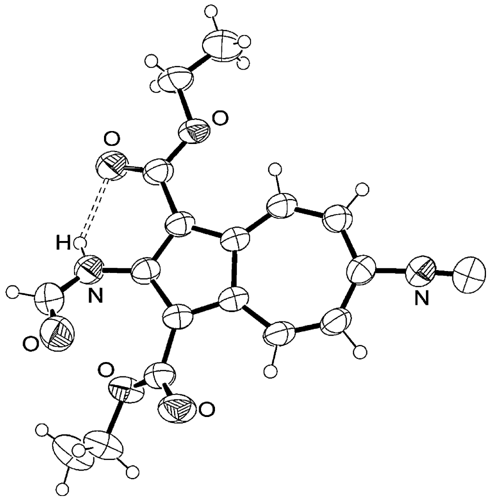

Fig. 18. ORTEP diagram of **9** [90].

7a/**b** and **8a**/**b** were obtained that show complexation of either of the inequivalent isocyanide termini of **5** (e.g., Fig. 17). For M = Cr, compounds **6a**, **7a**, and **8a** were produced in a statistical ratio (i.e., no complexation regioselectivity was observed), whereas minor preference for the complexation of the 2-isocyano end of **5** was noted for M = W. Remarkably, complexes **6a**/**b**, **7a**/**b**, and **8a**/**b** were easily separable by column chromatography on silica in neat dichloromethane and absolutely no scrambling of coordination (i.e., isomerization of **7** into **8**, **8** into **7**, or formation of **6**) was observed after refluxing THF solutions of the individual isomers **7** or **8** for 24 h.

Interestingly, when less than 1.0 equiv. of $POCl_3$ was administered drop-wise at 0 °C to dehydrate bisformamide **4** (Scheme 10), the essentially exclusive formation of 6-diisocyano-2-formamido-1,3-diethoxycarbonylazulene (**9**) was documented. The solid state conformation of **9** (Fig. 18) appears to be preserved in solution. The intramolecular H-bonding interaction in **4**, similar to that shown for **9** in Fig. 18, may be responsible for locking the conformation that obstructs access of the dehydrating agent to the 2-NHCHO end of **4**, thus resulting in significant suppression of the dehydration rate for the 2-NHCHO end of **4** compared to that for its 6-NHCHO end. The above behavior of **4** toward dehydration is consistent with our observation that the dehydrations of ^{6}AzNHCHO and ^{2}AzNHCHO proceed significantly faster compared to that of 1,3-diethoxycarbonyl-substituted ^{2}AzNHCHO [90].

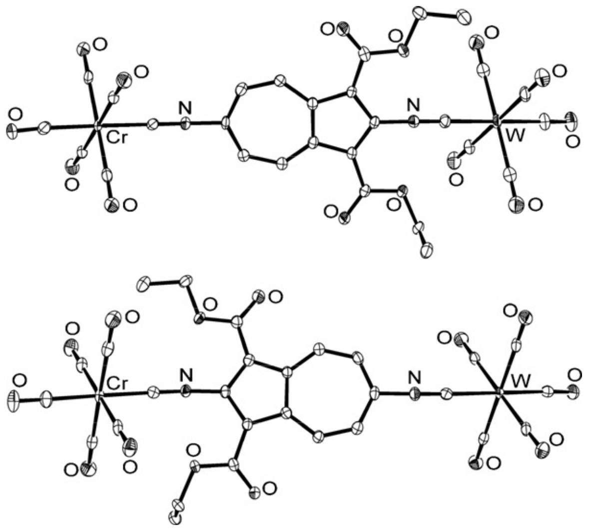

Fig. 19. ORTEP diagram of **11a** (top) and **11b** (bottom). Hydrogen atoms are omitted [90].

The access to 6-isocyano-2-formamide **9** in high yield provided a convenient route for efficient regioselective installation and complexation of the isocyanide junctions of **5** as shown in Scheme 10 for the synthesis of the Cr/W heterobimetallic complex **11a**. The isomer of **11a** with the interchanged Cr/W sites (**11b**) (Fig. 19) can be prepared simply by reversing the order of addition of the two $M(CO)_5(THF)$ reactants in Scheme 10. It is important to emphasize that the scope of the above strategy for synthesizing heterobimetallic adducts of **5** with controlled orientation of the azulenic dipole is limited by the tolerance of mononuclear species akin to **10** toward dehydration reaction conditions.

Despite the asymmetric nature of the 2,6-diisocyanoazulene motif **5**, the mononuclear isomers **7a** and **8a** exhibit the metal-to-ligand charge-transfer (MLCT, L = **5**) transitions of virtually identical energies. The same is true for the pair **7b**/**8b**. Binucleation of the mononuclear complexes of **5** (i.e., **7a** or **8a** → **6a**; **7b** or **8b** → **6b**) results in large red shifts of these MLCT bands, which clearly implies involvement of the entire 2,6-diisocyanoazulene unit (not just the NC junctions) in the charge transfer. The data in Table 2 show that the nonbenzenoid π system of **5** provides greater response in sensing complexation of the second NC junction compared to that of the analogous 1,4-diisocyanobenzene-bridged system [91] described earlier by Bennett and co-workers.

Also noteworthy is the fact that the metal-to-diisocyanide charge transfers for complexes **6**–**11** have remarkably low energies in context of the diisocyanoarene-bridged ensembles. For instance, the λ_{max} and ν_{max} of this MLCT band for the binuclear tungsten–diisocyanoazulene complex **6b** in CH_2Cl_2 are 515 nm

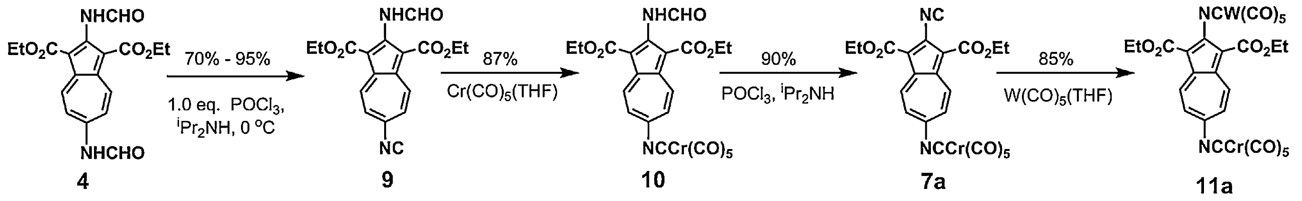

Scheme 10.

Table 2
Red shifts (ΔE_{MLCT}, L = diisocyanoarene) occurring upon binucleation of **5** or 1,4-diisocyanobenzene (DIB). Adapted with permission from Ref. [90].

Binucleation process	$\Delta E_{\mathrm{MDICT}}$, cm^{-1}
7a/8a → **6a**	≈1650[a]
7b/8b → **6b**	2042[a]
$(OC)_5W(\eta^1\text{-DIB}) \rightarrow [(OC)_5W]_2(\eta^1{:}\eta^1\text{-DIB})$	1221[b]

[a] Ref. [90].
[b] Ref. [91].

and 19,417 cm^{-1}, respectively, whereas those for the analogous diisocyanobenzene-linked species $[(CO)_5W]_2(\mu\text{-}1,4\text{-}CNC_6H_4NC)$ are 370 nm and 27,027 cm^{-1}.

Concurrently with the development of the 2,6-diisocyanoazulene-bridged systems, we also engaged in collaboration with the Chisholm group to consider carboxylate junctions for linking metal–metal quadruply bonded units through the 2,6-azulenic framework (Fig. 20) [92]. From the electron delocalization perspective, the mixed-valence ensembles generated by one-electron oxidation of structures such as **12** in Fig. 20 are more amenable to *quantitative* spectroscopic analysis than the classic "$t_{2g}{}^5$–bridge–$t_{2g}{}^6$" systems due to relative simplicity of the M(dδ) → L(pπ*) interaction vs. M(dπ) → L(pπ*) back-bonding (the latter involves several d-orbitals of π symmetry) [92]. For M = W, the strongly coupled (Class III), metal-based radical-cation, **12b**$^{+\bullet}$, featuring a nearly 14 Å-long separation between the M_2 termini was documented by the Chisholm and Dalal groups through a comprehensive series of spectroscopic and theoretical studies [92]. The unpaired electron is delocalized over all four W-atoms within **12b**$^{+\bullet}$, albeit unequally because of asymmetry of the 2,6-azulenic bridge [92]. One-electron reduction of complex **13** (Fig. 20), which involves a W–W quadruply bonded fragment ligated by two mutually *trans* 2-azulenecarboxylate ligands, provided a complementary mixed-valence scenario [93]. The thermally unstable, azulene-based radical-anion **13**$^{-\bullet}$ exhibits strong coupling between the two azulenic π systems mediated by the ligand(pπ)–W_2(dδ)–ligand(pπ) interaction.

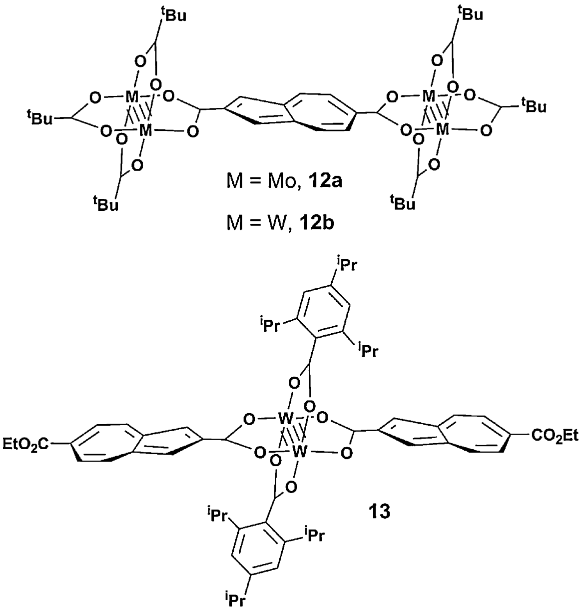

Fig. 20. 2,6-Azulene-dicarboxylate-bridged ensembles **12** (top) and their complementary system **13**.

5. Diisocyanoferrocene and its coordination complexes

In 2001, Hessen and van Leusen described a reasonably convenient, multigram preparation of 1,1′-diisocyanoferrocene from 1,1′-diisocyanatoferrocene (Scheme 11) [71]. The diisocyanate precursor is easily accessible from 1,1′-ferrocenedicarboxylic acid [94]. A more traditional route to 1,1′-diisocyanoferrocene would have involved formylation of 1,1′-diaminoferrocene followed by

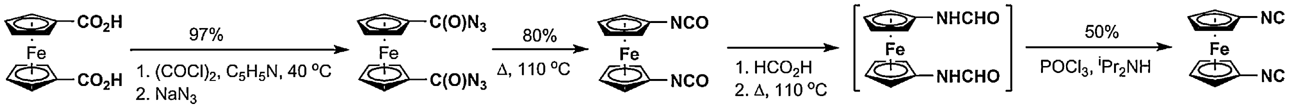

Scheme 11.

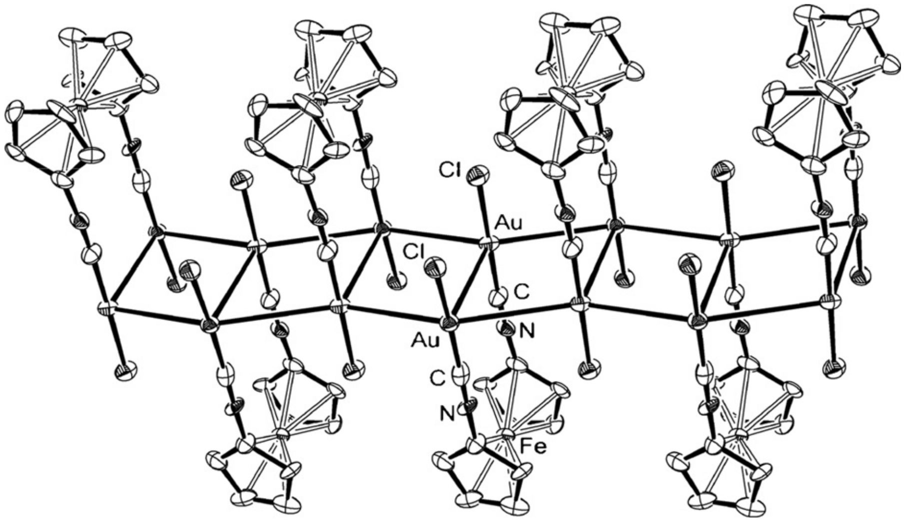

Fig. 21. ORTEP diagram of a fragment of the one-dimensional polymer $[(ClAu)_2(\mu\text{-}1,1'\text{-diisocyanoazulene})]_\infty$ generated using the CIF file provided in Ref. [96]. Hydrogen atoms are omitted.

double dehydration of the corresponding diformamide but the diamine had been an ill-defined substance at the time [71]. Since then, a greatly improved synthesis and structural characterization of 1,1′-diaminoferrocene was reported by Arnold et al. [95]. However, it remains to be seen whether the (still hypothetical) formylation/dehydration route to 1,1′-diisocyanoferrocene from 1,1′-diaminoferrocene would be competitive with the above Hessen's synthesis of this nonbenzenoid diisocyanide.

The coordination chemistry of 1,1′-diisocyanoferrocene debuted in 2005, when Siemeling et al. communicated on the structurally characterized complexes $[(OC)_5Cr]_2(\mu\text{-}1,1'\text{-diisocyanoferrocene})$ and $(ClAu)_2(\mu\text{-}1,1'\text{-diisocyanoferrocene})$ [96]. The former exhibits a synclinal orientation of the "$(OC)_5Cr(NC)$" moieties with respect to the 1,1′-ferrocene scaffold while the latter features an eclipsed geometry of the isocyanocyclopentadienyl rings and constitutes an elegant one-dimensional polymer, in which the monomeric units are held together by means of aurophilic interactions (Fig. 21) [96,97]. The motif shown in Fig. 21 may serve as an attractive initial experimental model for understanding adsorption of 1,1′-diisocyanoferrocene on metallic gold surfaces [96,98].

Other complexes of 1,1′-diisocyanoferrocene described by Siemeling et al. include $[Ag_2(\mu\text{-}1,1'\text{-diisocyanoferrocene})][NO_3]_2{\cdot}H_2O$ [98] as well as several of its adducts with dinuclear gold(I) acetylides $[\{Au(C{\equiv}C\text{—}\textit{para}\text{-}C_6H_4R)\}_2(\mu\text{-}1,1'\text{-diisocyanoferrocene})]$ (R = H, NMe_2, OMe) [97]. Surprisingly, the reaction between 1,1′-diisocyanoferrocene and $[Au(C{\equiv}CFc)]_n$ led to a highly unusual, and certainly unexpected, hexanuclear gold ensemble $[(\eta^5\text{-}FcC{\equiv}C\text{—}Au\text{—}C{\equiv}N\text{—}C_5H_4)Fe(\eta^5\text{-}C_5H_4\text{—}N{=}C\{Au\}\text{—}C{\equiv}CFc)]_3$ (Fig. 22) in a 72% yield [99]. Because the chemically identical isocyanide groups of the 1,1′-diisocyanoferrocene ligand underwent two drastically different types of reactions to form the Au_6 cluster (a simple coordination to a gold atom vs. an insertion of the isocyanide carbon atom into a gold–acetylide bond), Siemeling et al. provocatively termed this inexplicable and unprecedented reactivity as "schizoid" in the title of the their original communication [99].

6. Self-assembled monolayers (SAMs) of nonbenzenoid aromatic isocyanides on gold(1 1 1) surfaces

Exposure of freshly prepared gold films to CH_2Cl_2 solutions of various derivatives of isocyanoazulenes and diisocyanoazulene shown in Fig. 23 affords well-defined, self-assembled monolayers of these nonbenzenoid aryl isocyanides. The SAMs invariably exhibit upright η^1 coordination of the isocyanoazulene molecules to the gold(1 1 1) surface through their terminal isocyanide carbon atom, as established by grazing incidence reflection absorption FTIR and optical ellipsometry for each of the cases depicted in Fig. 23 [56]. For example, Fig. 24 illustrates FTIR changes in the ν_{CN} and ν_{CO} stretching regions that occur upon chemisorption of compound **8a** (Fig. 17) from its CH_2Cl_2 solution to the Au(1 1 1) surface.

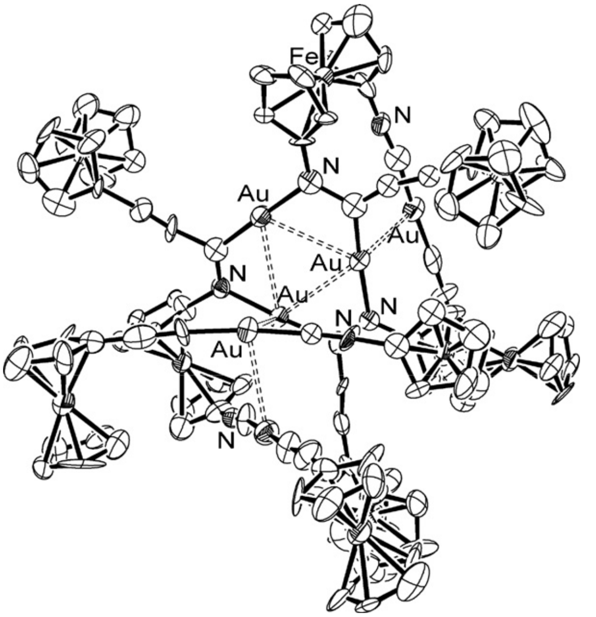

Fig. 22. ORTEP diagram of the hexanuclear gold cluster $[(\eta^5\text{-}FcC{\equiv}C\text{—}Au\text{—}C{\equiv}N\text{—}C_5H_4)Fe(\eta^5\text{-}C_5H_4\text{—}N{=}C\{Au\}\text{—}C{\equiv}CFc)]_3$ generated using the CIF file provided in Ref. [98]. Hydrogen atoms are omitted.

The solution FTIR spectrum of **8a** features ν_{CN} bands at 2115 and 2135 cm^{-1}, which correspond to stretching vibrations of the "free" 6-isocyano substituent and the 2-isocyano group coordinated to the Cr center, respectively (Fig. 24, top). The intense bands at 2043 cm^{-1} (A_1) and 1962 cm^{-1} (E) are due to ν_{CO} vibrations of the $[Cr(CO)_5]$ unit [90]. Upon adsorption to the Au surface, the peak at 2115 cm^{-1} is completely replaced by a new band at 2174 cm^{-1} (Fig. 24, bottom). Since the terminal carbon atom's lone pair is somewhat antibonding with respect to the C≡N bond [12], the isocyanide binding to the Au(1 1 1) surface in the upright η^1 fashion is accompanied by the shift of ν_{CN} to a higher frequency. The changes in relative intensities of the ν_{CO} bands for **8a** that occur upon the SAM formation are also indicative of a roughly perpendicular orientation of the molecules of **8a** to the metal surface [56]. In addition, the ellipsometric thickness of 18(2) Å measured for this monolayer is in full accord with the expected thickness of 17 Å, if the upright η^1 coordination of **8a** to the gold surface is assumed.

Interestingly, comparison of the solution and surface FTIR spectra for the 2,6-diisocyanoazulene **5** with the corresponding patterns for 2-isocyano-1,3-diethoxycarbonylazulene and 6-isocyano-1,3-diethoxycarbonylazulene indicates that **5** undergoes preferred, if not exclusive, binding to the gold surface via its 2-NC terminus (i.e., as drawn in Fig. 23). This is consistent with the 2-isocyano end of **5** being a somewhat stronger *net* electron donor than its 6-isocyano

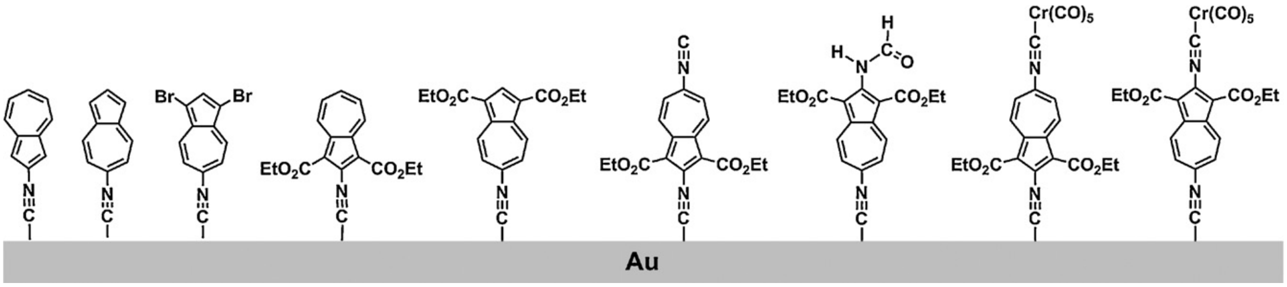

Fig. 23. The family of various 2- and 6-isocyanoazulenes, for which SAMs featuring upright η^1 coordination of the aryl isocyanide molecules to the gold(1 1 1) surface have been formed [56].

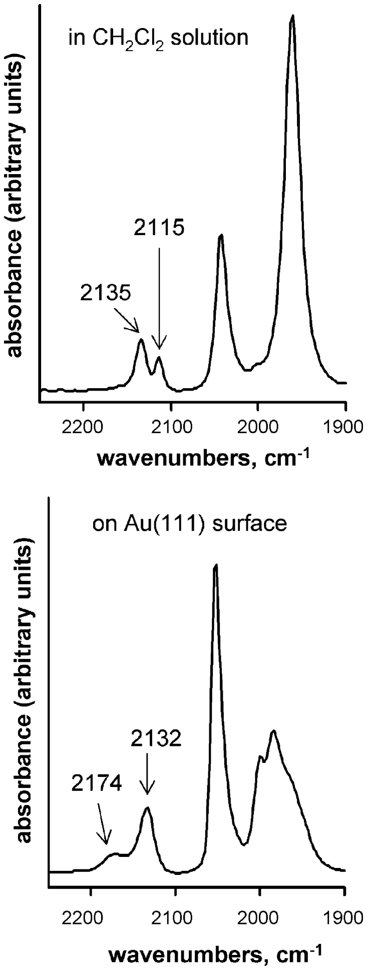

Fig. 24. FTIR spectra of compound **8a** (see Fig. 17) in a dichloromethane solution (top) and adsorbed to the gold surface (bottom) [56].

end, as suggested by the IR and ^{13}C NMR characteristics of **5–11** [90] and the redox properties of $Cr(CN^xAz)_6$ ($x = 2, 6$) [42].

The experimental accessibility of isocyanoazulenic SAMs already stimulated theoretical studies of such ensembles. The first computational (DFT and Molecular Dynamics) report in this regard addressed self-assembly of CN^2Az and its 1,3-diethoxycarbonyl-substituted derivative on Au(1 1 1) and concluded that these isocyanoazulenes could form ordered face-to-edge SAMs with vertical orientation of the adsorbed molecules with respect to the gold surface [100].

All of the isocyanoazulenic SAMs, schematically represented in Fig. 23, were prepared in air atmosphere and most did not deteriorate significantly following their storage without protection from air for at least a few weeks. In contrast, typical SAMs of aryl isocyanides on Au(1 1 1) should be prepared and stored under an inert atmosphere as they readily undergo decomposition via gold-promoted oxidation [101] of the isocyanide junctions to form isocyanates (R—N=C=O), if exposed to air [102,103]. A recently encountered exception involves adsorption of 8,16,24,32-tetraisocyano[2.2.2.2]metacyclophane to the Au(1 1 1) surface [104]. We have demonstrated that these films exhibit enhanced kinetic stability toward oxidation because they essentially feature four chemisorbed isocyanoarene moieties linked together through the aryl substituents [104].

Recently, Siemeling and co-workers described the formation and thorough characterization of well-ordered SAMs of 1,1′-diisocyanoferrocene on gold(1 1 1) [96,98]. Both isocyanide groups of this molecule undergo upright η^1 coordination to the gold surface, upon which the ν_{CN} band shifts from 2118 cm^{-1} for the free diisocyanide to 2181 cm^{-1} for the bidentate adsorbate. The dipodal mode of adsorption of the 1,1′-diisocyanoferrocene framework was also confirmed by X-ray photoelectron spectroscopy (XPS), which revealed only one N 1s emission [98]. The average tilt of the isocyanide group with respect to the gold surface was determined to be about 36° by means of near-edge X-ray absorption fine structure spectroscopy (NEXAFS).

7. Concluding remarks

The isocyanoazulene chemistry reviewed herein should greatly facilitate capitalizing on the unusual physicochemical characteristics of the azulenic framework in new coordination, organometallic, and surface settings. Isocyanoazulenes, such as CN^2Az and CN^4Az, proved to be stronger *net* electron acceptors as compared to conventional benzenoid aryl isocyanides, so their availability may be instrumental for accessing new stable isocyanometallates, which would further narrow the fundamental gap between carbon monoxide and organic isocyanides at the electron-rich extreme of the chemistries of these ligands. The 2,6-diisocyanoazulene motif appears to be an attractive platform for fabricating new types of azulene-based nanoarchitectures for their ultimate inclusion in molecular charge transport devices. The properties of η^5-isocyanocyclopentadienides can be tuned to a substantial degree by changing the metal fragment bound to the five-membered aromatic ring. The potential redox addressability of the isocyanoferrocene and 1,1′-diisocyanoferrocene moieties in both molecular and surface applications is intriguing. In addition, planar-chiral functionalization of the η^5-stabilized isocyanocyclopentadienide ligands may be envisioned [105].

Acknowledgments

This article is dedicated to Professor John E. Ellis of the University of Minnesota whose creativity and passion for chemistry have been a powerful source of inspiration to the author for over 15 years. The author is immensely grateful to his students and collaborators who have been involved in the research reviewed herein and whose names appear in the corresponding references. The author is particularly indebted to Professor Cindy L. Berrie for her critical role in taking the surface chemistry of isocyanoazulenes off the ground. Financial support by the National Science Foundation (CAREER Award CHE-0548212), DuPont (Young Professor Award), Kansas NSF EPSCoR, Kansas Technology Enterprise Corporation, and the University of Kansas is gratefully acknowledged as well. All thermal ellipsoid plots featured in this review were generated using the ORTEP-3 program (Version 2.02).

References

[1] W. Lieke, Justus Liebigs Ann. Chem. 112 (1859) 316.
[2] I. Ugi, Isonitrile Chemistry, Academic Press, New York, 1971.
[3] A. Gautier, Justus Liebigs Ann. Chem. 151 (1869) 239.
[4] W. Rothe, Pharmazie 5 (1950) 190.
[5] M.J. Garson, J.S. Simpson, Nat. Prod. Rep. 21 (2004) 164.
[6] C.W.J. Chang, Prog. Chem. Org. Nat. Prod. 80 (2000) 1.
[7] C.W.J. Chang, P.J. Scheuer, Top. Curr. Chem. 167 (1993) 33.
[8] A. Domling, Chem. Rev. 106 (2006) 17.
[9] L. Malatesta, Prog. Inorg. Chem. 1 (1959) 283.
[10] M. Meier, B. Mueller, C. Ruechardt, J. Org. Chem. 52 (1987) 648.
[11] E. Singleton, H.E. Oosthuizen, Adv. Organomet. Chem. 22 (1983) 209.
[12] P.M. Triechel, Adv. Organomet. Chem. 11 (1973) 21.
[13] Y. Yamamoto, Coord. Chem. Rev. 32 (1980) 193.
[14] E.M. Carnahan, J.D. Protasiewicz, S. Lippard, Acc. Chem. Res. 26 (1993) 90.
[15] F.E. Hahn, Angew. Chem., Int. Ed. Engl. 32 (1993) 650.
[16] R.J. Puddephatt, Coord. Chem. Rev. 216–217 (2001) 313.
[17] T. Nakano, Y. Okamoto, Chem. Rev. 101 (2001) 4013.

[18] S. Hong, R. Reifenberger, W. Tian, S. Datta, J. Henderson, C.P. Kubiak, Superlattice Microstruct. 28 (2000) 289.

[19] G. Heimel, L. Romaner, E. Zojer, J.-L. Bredas, Acc. Chem. Res. 41 (2008) 721.

[20] V. Sharma, D. Piwnica-Worms, Chem. Rev. 99 (1999) 2545.

[21] For a recent example, see: L.A. Labios, M.D. Millard, A.L. Rheingold, J.S. Figueroa, J. Am. Chem. Soc. 131 (2009) 11318.

[22] M.V. Barybin, W.W. Brennessel, B.E. Kucera, M.E. Minyaev, V.J. Sussman, V.G. Young Jr., J.E. Ellis, J. Am. Chem. Soc. 129 (2007) 1141.

[23] W.W. Brennessel, J.E. Ellis, Angew. Chem., Int. Ed. Engl. 46 (2007) 598.

[24] P.A. Leach, S.J. Geib, J.A. Corella, G.F. Warnock, N.J. Cooper, J. Am. Chem. Soc. 1116 (1994) 8566.

[25] T.L. Utz, P.A. Leach, S.J. Geib, N.J. Cooper, Chem. Commun. (1997) 847.

[26] M.V. Barybin, V.G. Young Jr., J.E. Ellis, J. Am. Chem. Soc. 122 (2000) 4678.

[27] J.A. Corella, R.L. Thompson, N.J. Cooper, Angew. Chem., Int. Ed. Engl. 31 (1992) 83.

[28] F. Wang, Y.-H. Lai, M.Y. Han, Macromolecules 37 (2004) 3222.

[29] F.X. Redl, O. Köthe, K. Röckl, W. Bauer, J. Daub, Macromol. Chem. Phys. 201 (2000) 2091.

[30] S. Schmitt, M. Baumgarten, J. Simon, K. Hafner, Angew. Chem., Int. Ed. Engl. 37 (1998) 1077.

[31] R.S.H. Liu, A.E. Asato, J. Photochem. Photobiol. C 4 (2003) 179.

[32] P.G. Lacroix, I. Malfant, G. Iftime, A.C. Razus, K. Nakatani, J.A. Delaire, Chem.-Eur. J. 6 (2000) 2599.

[33] R. Herrmann, B. Pedersen, G. Wagner, J.-H. Youn, J. Organomet. Chem. 571 (1998) 261.

[34] B.L. Feringa, R.A. van Delden, N. Koumura, E.M. Geertsema, Chem. Rev. 100 (2000) 1789.

[35] S.E. Estdale, R. Brettle, D.A. Dunmur, C.M. Marson, J. Mater. Chem. 7 (1997) 391.

[36] S. Ito, H. Inabe, N. Morita, K. Ohta, T. Kitamura, K. Imafuku, J. Am. Chem. Soc. 125 (2003) 1669.

[37] H. Salman, Y. Abraham, S. Tal, S. Meltzman, M. Kapon, N. Tessler, S. Speiser, Y. Eichen, Eur. J. Org. Chem. (2005) 2207.

[38] T. Zielinski, M. Kedziorek, J. Jurczak, Tetrahedron Lett. 46 (2005) 6231.

[39] M.J.S. Dewar, The Molecular Orbital Theory of Organic Chemistry, McGraw-Hill, New York, 1969.

[40] S.V. Shevyakov, H. Li, R. Muthyala, A.E. Asato, J.C. Croney, D.M. Jameson, R.S.H. Liu, J. Phys. Chem. A 107 (2003) 3295.

[41] R.S.H. Liu, J. Chem. Educ. 79 (2002) 183.

[42] R.E. Robinson, T.C. Holovics, S.F. Deplazes, D.R. Powell, G.H. Lushington, W.H. Thompson, M.V. Barybin, Organometallics 24 (2005) 2386.

[43] K. Kurotobi, H. Tabata, M. Miyauchi, R.A.F.M. Mustafizur, K. Migita, T. Murafuji, Y. Sugihara, H. Shimoyama, K. Fujimori, Synthesis (2003) 30.

[44] T. Shibasaki, T. Ooishi, N. Yamanouchi, T. Murafuji, K. Kurotobi, Y. Sugihara, J. Org. Chem. 73 (2008) 7971.

[45] K. Kurotobi, M. Miyauchi, K. Takakura, T. Murafuji, Y. Sugihara, Eur. J. Org. Chem. (2003) 3663.

[46] T. Morita, N. Abe, K. Takase, J. Chem. Soc., Perkin Trans. 1 (2000) 3063.

[47] M.R. Churchill, Prog. Inorg. Chem. 11 (1970) 53.

[48] S. Tofke, U. Behrens, Angew. Chem., Int. Ed. Engl. 26 (1987) 147.

[49] I.L. Fedushkin, M.N. Bochkarev, S. Mühle, H. Schumann, Russ. Chem. Bull., Int. Ed. 52 (2003) 2005.

[50] T.D. Lash, Eur. J. Org. Chem. (2007) 5461.

[51] R.E. Bulo, A.W. Ehlers, F.J.J. De Kanter, M. Schakel, M. Lutz, A.L. Spek, K. Lammertsma, B. Wang, Chem. Eur. J. 10 (2004) 2732.

[52] M. Iyoda, T. Kondo, T. Okabe, H. Matsuyama, S. Sasaki, Y. Kuwatani, Chem. Lett. 1 (1997) 35.

[53] A.H.M. Elwahy, K. Hafner, Tetrahedron Lett. 41 (2000) 2859.

[54] T. Farrell, T. Meyer-Friedrichsen, M. Malessa, D. Haase, W. Saak, I. Asselberghs, K. Wostyn, K. Clays, A. Persoons, J. Heck, A.R. Manning, J. Chem. Soc., Dalton Trans. (2001) 29.

[55] R.E. Robinson, T.C. Holovics, S.F. Deplazes, G.H. Lushington, D.R. Powell, M.V. Barybin, J. Am. Chem. Soc. 125 (2003) 4432.

[56] D.L. DuBose, R.E. Robinson, T.C. Holovics, D.R. Moody, E.C. Weintrob, C.L. Berrie, M.V. Barybin, Langmuir 22 (2006) 4599.

[57] A.G. Anderson Jr., R. Scotoni Jr., E.J. Cowles, C.G. Fritz, J. Org. Chem. 22 (1957) 1193.

[58] K. Hafner, K. Moritz, Justus Liebigs Ann. Chem. 656 (1962) 40.

[59] M. Mąkosza, P.W. Osiński, S. Ostrowski, Pol. J. Chem. 75 (2001) 275.

[60] M. Mąkosza, R. Podraza, Eur. J. Org. Chem. (2000) 193.

[61] T. Nozoe, S. Matsumura, Y. Murase, S. Seto, Chem. Ind. (London) (1955) 1257.

[62] K. Takase, T. Nozoe, T. Nakazawa, S. Fukuda, Tetrahedron 27 (1971) 3357.

[63] Y.-M. Lim, H.-S. Park, S.-H. Song, C.-J. Park, H. Ryu, J.-G. Jee, H.-S. Yang, Bull. Korean Chem. Soc. 20 (1999) 701.

[64] O.I. Mikhailova, G.A. Dushenko, I.E. Mikhailov, R.M. Minyaev, V.I. Minkin, Russ. J. Org. Chem. 44 (2008) 1451.

[65] K. Banert, F. Koehler, B. Meier, Tetrahedron Lett. 44 (2003) 3781.

[66] G.R. Knox, P.L. Pauson, D. Willison, E. Solcániová, Š. Toma, Organometallics 9 (1990) 301.

[67] T. El-Shihi, F. Siglmüller, R. Herrmann, M.F.N.N. Carvalho, A.J.L. Pombeiro, J. Organomet. Chem. 335 (1987) 239.

[68] T. El-Shihi, F. Siglmüller, R. Herrmann, M.F.N.N. Carvalho, A.J.L. Pombeiro, Port. Electrochim. Acta 5 (1987) 179.

[69] M.V. Barybin, T.C. Holovics, S.F. Deplazes, G.H. Lushington, D.R. Powell, M. Toriyama, J. Am. Chem. Soc. 124 (2002) 13668.

[70] B. Bildstein, M. Malaun, H. Kopacka, K. Wurst, M. Mitterböck, K.-H. Ongania, G. Opromolla, P. Zanello, Organometallics 18 (1999) 4325.

[71] D. van Leusen, B. Hessen, Organometallics 20 (2001) 224.

[72] K. Kavallieratos, S. Hwang, R.H. Crabtree, Inorg. Chem. 38 (1999) 5184.

[73] A.G. Ginzburg, Russ. Chem. Rev. 62 (1993) 1098.

[74] T.C. Holovics, S.F. Deplazes, M. Toriyama, D.R. Powell, G.H. Lushington, M.V. Barybin, Organometallics 23 (2004) 2927.

[75] M. Cais, N. Narkis, J. Organomet. Chem. 3 (1965) 188.

[76] M.K. Pomije, C.J. Kurth, J.E. Ellis, M.V. Barybin, Organometallics 16 (1997) 3582.

[77] E.P. Kündig, P.L. Timms, J. Chem. Soc., Dalton. Trans. (1980) 991.

[78] E. Ljungström, Acta Chem. Scand. A32 (1978) 47.

[79] D.A. Bohling, K.R. Mann, Inorg. Chem. 23 (1984) 1426.

[80] W.S. Mialki, D.E. Wigley, T.E. Wood, R.A. Walton, Inorg. Chem. 21 (1982) 480.

[81] J.P. Bullock, K.R. Mann, Inorg. Chem. 28 (1989) 4006.

[82] P.M. Treichel, G.J. Essenmacher, Inorg. Chem. 15 (1976) 146.

[83] S.F. Deplazes, Ph.D. Thesis, The University of Kansas, 2007.

[84] A.N. Nesmeyanov, E.G. Perevalova, S.P. Gubin, K.I. Grandberg, A.G. Kozlovsky, Tetrahedron Lett. 22 (1966) 2381.

[85] B.E. Bursten, J. Am. Chem. Soc. 104 (1982) 1299.

[86] R.N. McDonald, R.R. Reitz, J. Org. Chem. 37 (1972) 2703.

[87] T.W. Ebbesen (Ed.), Carbon Nanotubes: Preparation and Properties, CRC Press Inc., Boca Raton, FL, 1997.

[88] V.H. Crespi, L.X. Benedict, M.L. Cohen, S.G. Louie, Phys. Rev. B 53 (1996) R13303.

[89] G. Treboux, P. Lapstun, K. Silverbrook, J. Phys. Chem. B 102 (1998) 8978.

[90] T.C. Holovics, R.E. Robinson, E.C. Weintrob, M. Toriyama, G.H. Lushington, M.V. Barybin, J. Am. Chem. Soc. 128 (2006) 2301.

[91] D.S. Grubisha, J.S. Rommel, T.M. Lane, W.T. Tysoe, D.W. Bennett, Inorg. Chem. 31 (1992) 5022.

[92] M.V. Barybin, M.H. Chisholm, N.S. Dalal, T.C. Holovics, N.J. Patmore, R.E. Robinson, D.J. Zipse, J. Am. Chem. Soc. 127 (2005) 15182.

[93] M.V. Barybin, M.H. Chisholm, N.J. Patmore, R.E. Robinson, N. Singh, Chem. Commun. (2007) 3652.

[94] P.M. Petrovitch, Double Liaison 133 (1966) 1093;
Chem. Abstr. 68 (1968) 29843s.

[95] A. Shafir, M.P. Power, G.D. Whitener, J. Arnold, Organometallics 19 (2000) 3978.

[96] U. Siemeling, D. Rother, C. Bruhn, H. Fink, T. Weidner, F. Traeger, A. Rothenberger, D. Fenske, A. Priebe, J. Am. Chem. Soc. 127 (2005) 1102.

[97] U. Siemeling, D. Rother, C. Bruhn, Organometallics 27 (2008) 6419.

[98] T. Weidner, N. Ballav, M. Zharnikov, A. Priebe, N.J. Long, R. Winter, A. Rothenberger, D. Fenske, D. Rother, C. Bruhn, H. Fink, U. Siemeling, Chem. Eur. J. 14 (2008) 4346.

[99] U. Siemeling, D. Rother, C. Bruhn, Chem. Commun. (2007) 4227.

[100] J.-H. Zhou, L.-W. Shi, T. Zhang, M.-B. Chen, Chin. J. Chem. 25 (2007) 1223.

[101] A.M. McDonagh, M.H. Zareie, M.J. Ford, C.S. Barton, M. Ginic-Markovic, J.G. Matisons, J. Am. Chem. Soc. 129 (2007) 3533.

[102] J.J. Stapleton, T.A. Daniel, S. Uppili, O.M. Cabarcos, J. Naciri, R. Shashidhar, D.L. Allara, Langmuir 21 (2005) 11061.

[103] S.A. Swanson, R. McClain, K.S. Lovejoy, N.B. Alamdari, J.S. Hamilton, J.C. Scott, Langmuir 21 (2005) 5034.

[104] M. Toriyama, T.R. Maher, T.C. Holovics, K. Vanka, V.W. Day, C.L. Berrie, W.H. Thompson, M.V. Barybin, Inorg. Chem. 47 (2008) 3284.

[105] S.F. Deplazes, T.C. Holovics, M.V. Barybin, in preparation.